Journal of Paleolimnology **28:** 219–236, 2002.

Reconstructing lake and drainage basin history using terrestrial sediment layers: analysis of cores from a post-glacial lake in New England, USA

Sarah Brown[1,4,*], Paul Bierman[1], Andrea Lini[1], P. Thompson Davis[2] and John Southon[3]
[1]Department of Geology, University of Vermont, Burlington, Vermont 05405, USA; [2]Natural Sciences, Bentley College, Waltham, Massachusetts 02452, USA; [3]Center for Accelerator Mass Spectrometry, Lawrence Livermore National Laboratory, Livermore, California 94551, USA; [4]Department of Geosciences, Oregon State University, Corvallis, Oregon 97331, USA; [*]Author for correspondence (e-mail: sarah.lewis@orst.edu)

Received 3 April 2001; accepted in revised form 15 November 2001

Key words: Event sedimentation, Holocene, Radiocarbon-based chronology, Storms, Watershed erosion

Abstract

Four sediment cores and twenty-five ^{14}C ages from Ritterbush Pond in northern Vermont provide a detailed and continuous temporal record of Holocene lake and watershed dynamics. Using visual logs, carbon content, magnetic susceptibility, stable isotope signatures, and X-radiography, all measured at 1-cm scale, we identify and date discrete layers of terrestrially-derived sediment in the organic-rich, lacustrine gyttja. These inorganic layers range in thickness from <1 mm to >10 cm and range in grain size and sorting from homogeneous silt to graded sand. AMS radiocarbon ages both from macrofossils within the thickest layers, and gyttja bracketing these layers, provide the basis for correlation among the cores, the dating of 52 basin-wide sedimentation events, and the development of a detailed sedimentation chronology for the Holocene.

Physical, chemical, and isotopic analyses suggest the inorganic layers are terrestrially derived and result from hydrologic events large enough to erode and transport sediment from the watershed into the pond. The temporal and spatial distribution of the inorganic layers suggests changing basin-wide sedimentation and thus erosion dynamics since deglaciation over 12,000 years ago. Specifically, for intervals lasting 400 to 1000 years, during the early ($>$8600 cal yBP), middle (6400 to 6800 cal yBP) and late Holocene (1800 to 2600 cal yBP), the Ritterbush Pond watershed eroded more rapidly than at other times and terrestrially derived material poured into the pond. Analysis of Ritterbush Pond sediments demonstrates the potential for North American lakes to preserve a record of drainage basin dynamics.

Introduction

The deposition of terrestrially-derived sediment in mountain lakes, and its significance to the reconstruction of lake histories and the interpretation of watershed dynamics, has received little attention in New England. Most lake research in the northeastern North America has focused on constructing vegetative histories from pollen data (Davis and Jacobson 1985; Jackson and Whitehead 1991; Spear et al. 1994; Spear 1989). These pollen chronologies have been used to characterize general changes in temperature and moisture in New England since deglaciation. With the exception of lake research related to the Younger Dryas climate oscillation (Thompson et al. 1996), deposits of inorganic sediment within lacustrine cores from the New England area have been treated as anomalous, basin-specific events (Davis 1969, 1999).

To demonstrate the importance of understanding the terrestrial sediment influx to mountain lakes, we have developed a radiocarbon-based chronology of Holocene sedimentation events for Ritterbush Pond, located in the north-central Green Mountains of Vermont (Figure 1,2). The events are recorded as discrete layers of inorganic sediment (sand and silt) within a core primarily composed of organic-rich gyttja (Fig-

ure 3). The inorganic layers in Ritterbush Pond are episodic, distinct, basin-wide deposits with variations in temporal distribution suggestive of changes in frequency of terrestrial sediment delivery to the lake since deglaciation over 12,000 years ago.

Bierman et al. (1997) correlated times of increased deposition of these inorganic layers in Ritterbush Pond to periods of regional hillslope erosion recorded by alluvial fans, and suggested a connection between inorganic sedimentation events, hillslope destabilization, and regional climate patterns. We interpreted the Ritterbush chronology as a record of paleostorm frequency and magnitude (Brown et al. 2000). This paper details the process by which we identifed and

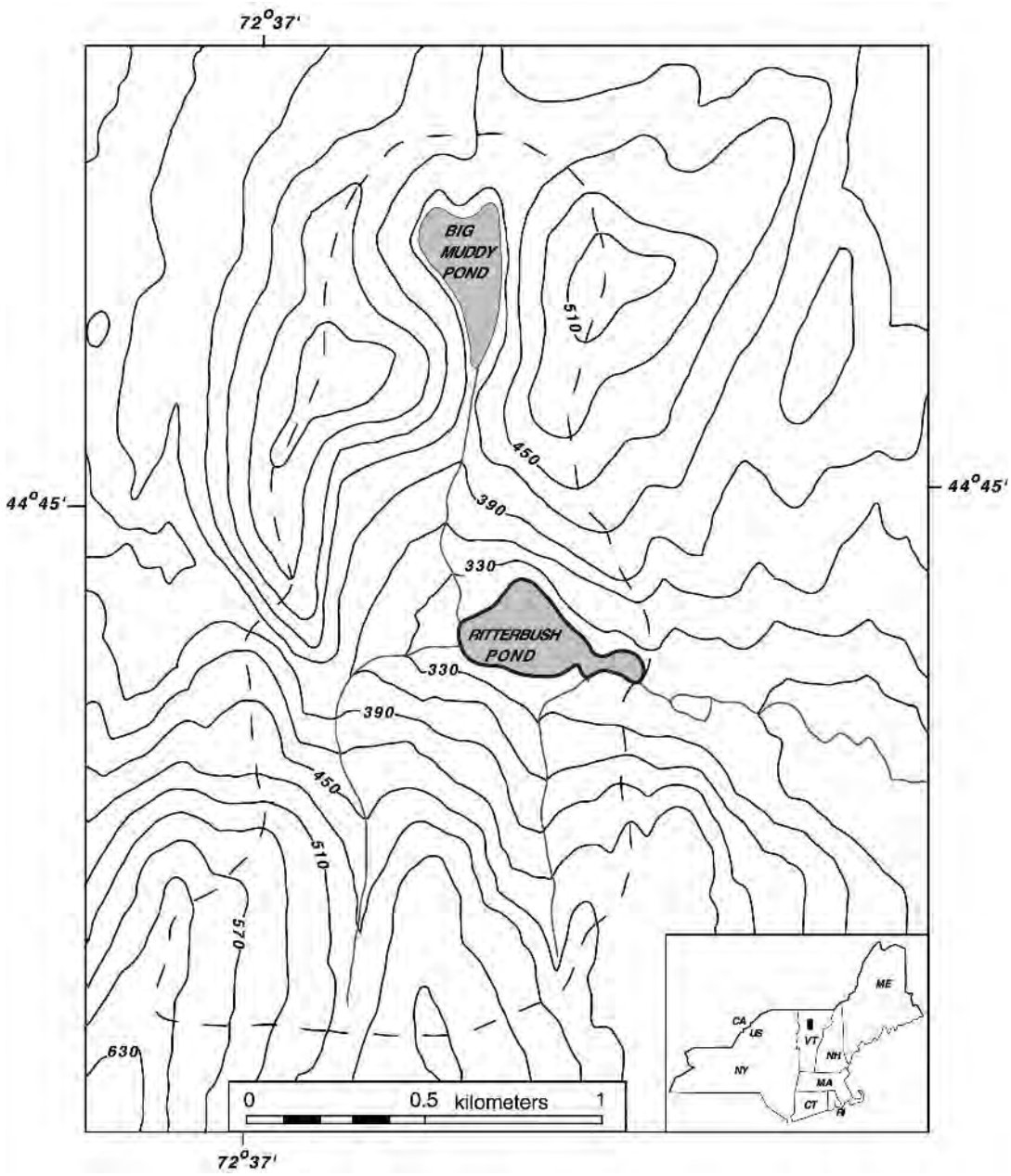

Figure 1. Ritterbush Pond watershed, Eden Vermont: watershed area, 2.2 km^2, pond elevation, 317 m; surface area, 0.07 km^2; maximum water depth 13.6 m. Dashed line indicates watershed boundary. Contour interval, 30 m. Adapted from U.S. Geological Survey Eden and Hazens Notch 7.5′ (1:24000) topographic quadrangle maps (1986).

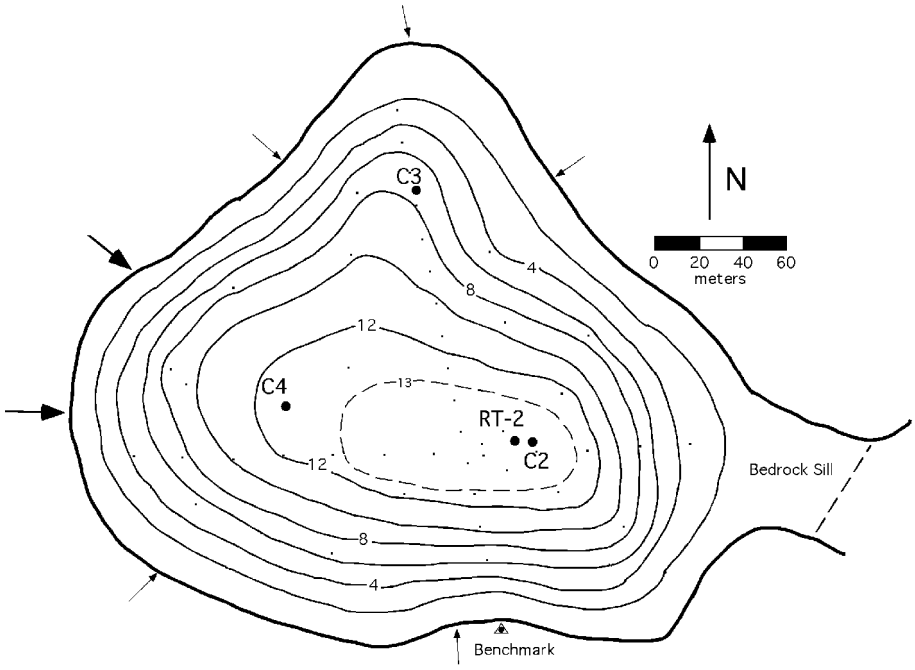

Figure 2. Ritterbush Pond bathymetry and core locations (bold dots). Contour interval is 2 m. Small dots indicate bathymetric data points. Broad arrows represent perennial stream inflow; smaller arrows denote intermittent streams.

characterized the inorganic sediment layers and thus created the event chronology for Ritterbush Pond.

Ritterbush Pond

Ritterbush Pond is a small, oligotrophic lake in the north-central Green Mountains of Vermont (Figure 1). The steep slopes of the forested watershed are underlain by schist and covered by a thin mantle of till and widely scattered deposits of stratified drift. Soils are classified as rocky and sandy loams of irregular thickness, with up to 10% bedrock exposure (Babcock 1979). The shoreline of Ritterbush Pond is generally shallow, sandy, and vegetated on the southern end, dominated by a marshy area on the western side, and bounded by steeper and rockier slopes to the northeast. The lake itself is bowl shaped, with a shallow lake margin, steep inner slopes, and a relatively flat bottom; maximum depth is 13.6 m (Figure 2). At the eastern end of the lake, the outlet is controlled by a shallow (0.5 m) bedrock sill. There are two major perennial streams that feed Ritterbush Pond at its western end. Both streams are incised to bedrock along the steep hillslopes, except where the channel gradient decreases, or woody debris blocks flow to form pools that collect sediment. The streams commonly run clear, suggesting little suspended load is carried to the lake during baseflow periods. We observed no evidence for large-scale mass movement, such as landslide scarps or debris flow deposits in the watershed. However, extensive and deeply incised deposits of gravel were observed near the outlet for Big Muddy Pond (A. Noren, pers. comm.), located upslope and to the north of Ritterbush Pond (Figure 1).

Previous research

Ritterbush Pond was previously cored to determine time of deglaciation from basal radiocarbon ages, and to obtain material for pollen and stable isotope research. A single core from the western end of the pond was used to construct a pollen chronology (Sperling et al. 1989), but the reported core stratigraphy is not sufficiently detailed for comparison with the cores analyzed for this research. A pair of overlapping, 2-inch Livingstone cores (cores RT-1 and RT-2) from the lake center showed distinct variations in organic carbon content, as approximated by loss on ignition (LOI), and provided the initial identification of the inorganic layers (Lin 1996). Lin (1996) hypoth-

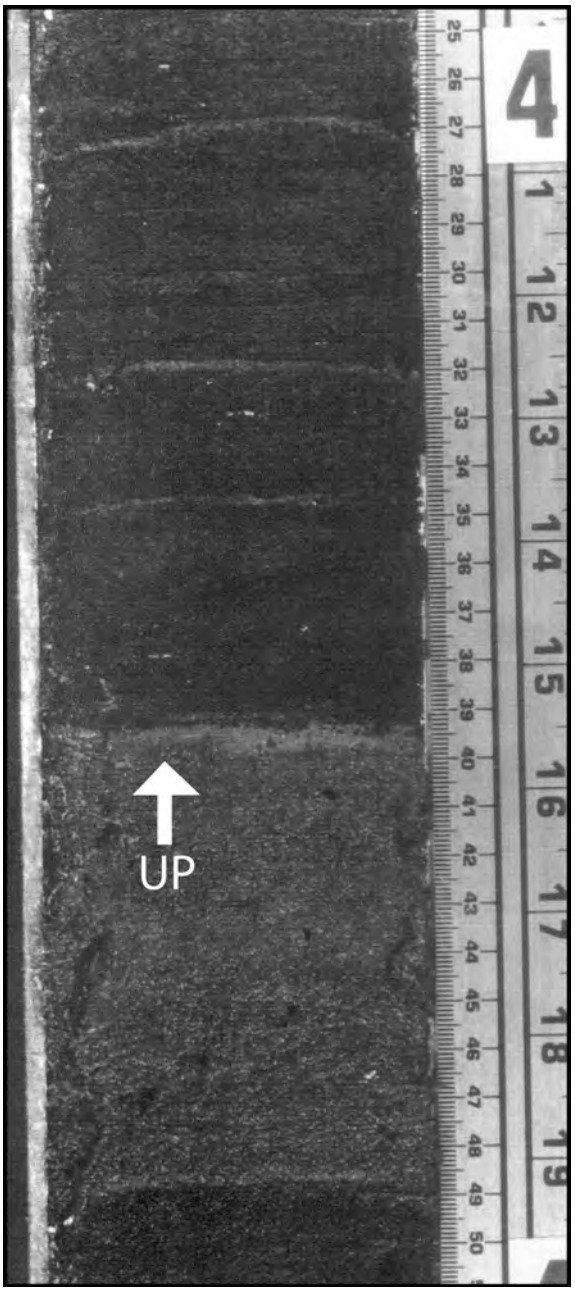

Figure 3. Photograph of core C2 showing a thick organic layer (q). The 10-cm thick brown inorganic layer has sharp upper and lower contacts with the surrounding black gyttja. Millimeter-scale gray/brown laminations are also visible (427, 432 and 434.5 cm depth).

esized that the inorganic layers were catastrophically deposited by sediment re-suspension due to flood or storm events. Five ^{14}C ages were obtained from bulk gyttja samples of the cores to construct a pollen-based deglacial and post-glacial vegetation and climate history for the Ritterbush watershed (Lin 1996).

Subsequent re-examination of cores RT-1 and RT-2 included stable isotope analysis and nine additional radiocarbon ages (Bierman et al. 1997). Systematic variations in $\delta^{13}C$ values with lithology were interpreted as indicating different source material for the gyttja (aquatic) and inorganic layers (terrestrial) (Lini et al. 1995). Three pairs of radiocarbon ages that bracket the thickest inorganic layers demonstrate that the terrestrially derived layers were deposited rapidly (Bierman et al. 1997). The stratigraphic log and loss-on-ignition (LOI) data for core RT-2, the 14 previously published radiocarbon ages, and the pollen chronology developed for the Ritterbush watershed are all presented here along with data from three new Ritterbush Pond sediment cores.

Core collection

We collected three additional sediment cores from Ritterbush Pond (Figure 2), one from the lake center (core C2) and two closer to the lake margin (cores C3 and C4). The cores were retrieved using a percussion coring device (Reasoner 1993), with a piston and a core-catcher (Figure 4). This inexpensive, lightweight, easily transportable system allowed us to retrieve up to 6 m of continuous, wide-diameter (7.5 cm) core working from the stable platform of the ice-covered lake. The cores were retrieved using a pulley system anchored in the ice to obtain mechanical advantage. In the field, the 6-m-long PVC pipe encasing the core was cut into shorter lengths ($<$1.5 m) for transport to the laboratory for sampling and storage.

Core lithology

Black, fine-grained, organic gyttja is the dominant core lithology. The gyttja is relatively homogenous within each core, and generally increases in coherency and firmness with depth. Fine sand and silt are present as discrete layers in all four cores. The inorganic layers can be divided into two types: thick (1–10 cm) graded and non-graded beds, and thin ($<$1 cm) laminations. The boundary between the gyttja and the inorganic material is generally sharp; however, the lower transition from gyttja to sand or silt in some of the thickest inorganic layers appears gradual. Evidence for bioturbation is present in the upper cm of only one of 52 inorganic layers identified in the

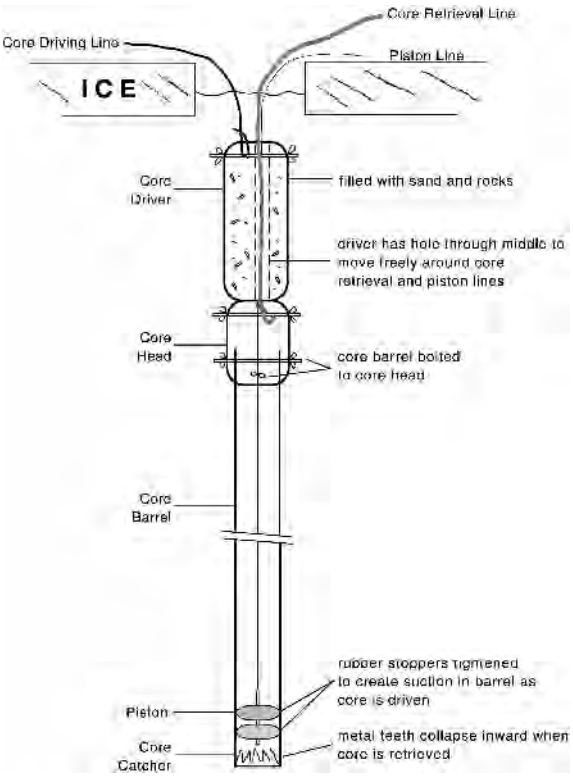

Figure 4. Modified Reasoner coring device used to retrieve sediment cores from Ritterbush Pond (Reasoner 1993).

central core (C2). Macrofossils (seeds, leaves, and woody particles) are found above, below and within the inorganic layers, as well as in the gyttja where distinct inorganic layers are absent.

Pollen analysis

The pollen record for Ritterbush Pond developed by Lin (1996) was based on a resolution of one sample every ten cm, along with standard preparation and counting procedures. In general, Ritterbush Pond reveals a vegetation and climate record similar to the New England pollen sequence of Davis (1969). The hemlock decline is recognized around 4800 ^{14}C yr BP. Thus, warm and moist conditions prevailed from about 9000 to 1600 ^{14}C yr BP, spanning all three intervals of increased inorganic layer deposition.

Laboratory analysis

Our laboratory procedures were designed to produce high-resolution (1 cm) measurements of physical, lithological, and isotopic properties of the sediment cores. These measurements were then compared within and between the cores to create a detailed sedimentation history for Ritterbush Pond, including an age model for gyttja accumulation and the deposition of individual inorganic layers.

Analyses on PVC-encased core segments

X-radiography and magnetic susceptibility analyses were used to identify the distribution and thickness of the inorganic layers prior to opening the core segments. Overlapping X-radiographs were taken of the core segments, scanned, matched, and measured for grayscale density at 72 dpi using imaging software. The density measurements were averaged and recorded for 1-cm intervals. Magnetic susceptibility was measured using a Bartington MS2 and an automated core-logging system. The coil generating and measuring the magnetic field integrates over 4 cm of the core and data were recorded at 1-cm intervals for the length of the each core.

Each core was also analyzed for paleomagnetic declination, inclination, and intensity using a cryogenic magnetometer. Other lake sediments have been shown to be excellent recorders of paleomagnetic secular variation (PSV) where the slow settling of clay-sized particles allows detrital magnetite to align with Earth's magnetic field. Secular variation of both declination and inclination has been used to correlate lake sediment records from deglacial and post-glacial lakes in New England, North America, and Europe (Lund 1996; Peck et al. 1996; Ridge et al. 1999). Due to the strong, probably current-laid orientation of magnetite grains in the inorganic layers and the 14-cm integration length of the measurement, the small-magnitude, low-intensity shifts associated with PSV were not discernible in the Ritterbush Pond cores; thus, no further use was made of these data.

Core processing

Each core segment was split lengthwise using a circular saw and a 1.8-m-long stainless steel blade. First, two saw cuts were made down the length of each core segment just through the $\frac{1}{4}''$ wall on opposite sides of the PVC tube. Then, the blade was inserted between the cuts to slice through the sediment and separate the core halves. The archival half was wrap-

Table 1. Radiocarbon ages for Ritterbush Pond.

CAMS #	Core	Depth (cm)	Correlation depth in C2	Material	$\delta^{13}C$ [a]	^{14}C age	Adjusted ^{14}C age[b]	Calibrated age (calendar yr B.P.)[c]	Best age estimate[d]
33132	RT-2	96	164	gyttja	−31.7	2570 ± 60	2120	2146 (2093) 1993	2090
33135	RT-2	142	228	gyttja	−31.5	3170 ± 60	2720	2855 (2787) 2767	2790
33352	RT-2	154	238	gyttja	−29.5	2940 ± 70	2490	2717 (2707, 2629, 2499) 2475	2610
22993	RT-2	220	300	gyttja	−30.6	3960 ± 60	3510	3843 (3817, 3782, 3732) 3700	3780
33351	RT-2	339	439	gyttja	−32.0	6540 ± 60	6090	7014 (6915) 6871	6920
20195	RT-2	348	448	gyttja	−32.4	6430 ± 70	5980	6884 (6833, 6826, 6799) 6742	6820
32856	RT-2	416	537	gyttja	−32.7	9140 ± 60	8690	9666 (9638) 9533	9640
32854	RT-2	426	547	gyttja	−31.8	8870 ± 60	8420	9469 (9434) 9374	9430
33134	RT-2	426	547	gyttja	−31.8	8950 ± 50	8500	9469 (9467) 9444	9470
33350	RT-2	426	547	gyttja	−31.8	8890 ± 60	8440	9471 (9440) 9385	9440
32855	RT-2	426	547	seed	−28	8450 ± 60	8450	9475 (9442) 9389	9440
46942	C2	77	77	gyttja	−31	1290 ± 40	840	771 (733) 699	730
46943	C2	383	383	gyttja	−31	5240 ± 40	4790	5587 (5578) 5566; 5540 (5510, 5505) 5473	5520
46944	C2	424	424	gyttja	−31	6080 ± 40	5630	6456 (6412) 6394	6410
40775	C2	439.7	439.7	twig	−28	6020 ± 70	6020	6932 (6866) 6767	6870
46945	C2	489	489	gyttja	−31	7720 ± 40	7270	8081 (8060, 8039) 8021; 8017 (8001) 7981	8030
40776	C2	548	548	gyttja	−31	9030 ± 60	8580	9571 (9505) 9459	9510
44693	C3	63.5	164	wood	−26.5	2050 ± 50	2050	2060 (1990) 1931	1990
44695	C3	144	238	wood	−27.6	2550 ± 50	2550	2751 (2726) 2709; 2622 and 2502	2610
44697	C3	375	432	wood	−28	5790 ± 70	5790	6677 (6626) 6504	6630
44699	C3	444	510	bark	−32.0	7880 ± 50	7880	8718 (8582) 8540	8580
44694	C4	81	164	leaves	−28.0	2040 ± 50	2040	2042 (1980) 1916	1980
44696	C4	132	238	gyttja, leaves	−29.5	2570 ± 60	2570[e]	2761 (2734) 2709; 2623 and 2502	2630
44698	C4	311	448	gyttja, leaves	−23.3	6430 ± 40	5980	6860 (6833, 6826, 6799) 6774	6820
44700	C4	380	547	wood	−30.6	8450 ± 50	8450	9473 (9442) 9399	9440

All ages are stratigraphically correlated to depth in core C2

[a]Measured acid-base-acid washed samples reported to one decimal place. Estimated values are average for all measured samples and have no decimal.

[b]^{14}C ages were adjusted for measured gyttja-macrofossil offset by subtracting 450 14C years from each gyttja age. For explanation and justification see Bierman et al. (1997).

[c]Adjusted ^{14}C ages calibrated using CALIB rev3.0.3A (Stuiver and Reimer 1993). A 1 σ range encloses reported intercepts in ().

[d]Intercept or average of intercepts where one range is reported, weighted average of intercepts (or midpoint of range where no intercept is reported) where 2 ranges are reported. Ages rounded to nearest decade.

[e]Sample not adjusted for gyttja-macrofossil because of ambiguity of material dated.

ped and stored immediately; the remaining half was prepared for logging and sampling.

Core photographs and graphic logs were prepared prior to core sampling and provide a visual record of core lithology. Each core was then dissected at 1-cm intervals and stored in 20-ml bottles to provide a homogeneous, easily stored, readily accessible sample for subsequent analyses. Prior to dissection of core C2, ten volumetric (1 cm^3) samples of gyttja were removed at approximately half-meter intervals for bulk density measurements used to calculate mass loading rates into the center of the pond.

Analyses of bottled sediment samples

Aliquots were removed from the sample bottles to assess the amount and type of organic matter with cm-by-cm resolution. Loss on ignition (LOI) and total organic carbon (TOC) provide estimates of percent organic matter in the sediment. Carbon/nitrogen ratios (C/N) and stable carbon isotopes ($\delta^{13}C$) suggest the source (terrestrial or aquatic) of the organic matter itself. LOI was measured (standard error $\pm 0.05\%$) as the percent weight lost to combustion at 450 °C for 2 hours, for all samples from each of the three cores. TOC and C/N were measured for core C2, using HCl-treated aliquots from all samples, on a CE NC 2500 Elemental Analyzer. Replicate samples give a standard error of $\pm 0.1\%$ for carbon and $\pm 0.05\%$ for nitrogen. Samples were measured for $\delta^{13}C$ by combustion of HCl-pretreated samples in quartz tubes, isolating the CO_2 on a vacuum line, and analyzing the gas with a VG SIRAII mass spectrometer. Stable carbon isotopes were measured on 20 samples selected from core C2, and on other samples used for radiocarbon dating for segments from all three cores (Table 1).

Samples from each core were also analyzed for mean grain size and percent charcoal content. The grain size of pretreated samples from selected inorganic layers in each of the three cores was measured using a Coulter Laser Diffraction Unit (LS 230). Percent charcoal for five inorganic layers and three sections of gyttja was estimated with a nitric acid digestion technique modified from (Winkler 1985). The samples were treated with concentrated nitric acid to oxidize organic material and then combusted using the Elemental Analyzer to determine TOC as a percent of the digested sample.

Radiocarbon dating

Methods

Samples of gyttja and macrofossils were removed for dating during core processing. Additional samples were removed subsequently from individual sample bottles. A total of 14 new samples were prepared for Accelerator Mass Spectrometer (AMS) radiocarbon dating at Lawrence Livermore National Laboratory using standard procedures. Samples received an acid-base-acid treatment (1N NCl, 1N NaOH, 80 °C) and were combusted in vacuo at 900 °C with CuO in sealed quartz tubes. The resulting CO_2 was cryogenically purified and reduced to graphite with hydrogen using an iron catalyst. Samples were measured repeatedly by AMS relative to aliquots of the NBS Oxalic Acid 1 standard (SRM 4990B), along with known-age secondary standards and coal process blanks. The AMS data were converted to ^{14}C ages using standard algorithms (Stuiver and Polach 1977; Donahue et al. 1990). For seven samples, acid/base treated sample material was measured for $\delta^{13}C$ to correct for isotopic fractionation of carbon; where treated sample material was unavailable, $\delta^{13}C$ was estimated as the average of the measured values ($-31‰$ for gyttja, $-28‰$ for macrofossils). The quoted errors represent the larger of propagated counting statistics and the scatter in the several measurement runs for each sample.

Interpretation of ages

The difference in radiocarbon ages of gyttja and macrofossils from the same stratigraphic horizon was tested at Ritterbush Pond (Bierman et al. 1997). At 426 cm depth in core RT-2, a macrofossil was dated at 8450 $\pm$ 60 ^{14}C yr BP, while the surrounding gyttja was dated at 8900 $\pm$ 40 ^{14}C yr BP, resulting in an age difference of 450 ^{14}C years. In other lakes, bulk ^{14}C ages of carbonate-free gyttja have also been shown to be hundreds of years (400 to 500 years) older than AMS ages of terrestrial plant fragments (Wohlfarth et al. 1993). This offset is commonly attributed to the lake reservoir effect caused by the introduction of old, ^{14}C -depleted carbon from bedrock, basal sediments, or groundwater, which lowers the $^{14}C/^{12}C$ ratio in the dissolved CO_2 used by algae and non-emergent plants comprising the gyttja (Olsson 1986). Thus, we account for the measured offset by subtracting 450 ^{14}C years from all of our gyttja radiocarbon ages.

Radiocarbon ages were calibrated to calendar years using CALIB rev3.0.3A (Stuiver and Reimer 1993). We interpreted the resulting intercepts and error ranges in the following manner: where one range is reported, we use the intercept or average of the intercepts; where two ranges are reported, we use a weighted average of intercepts, or weighted average of range midpoints where no intercept is reported. The weighted average was based on the reported probability of each intercept or range. Our estimate for each calendar age equivalent of each ^{14}C age is reported to the nearest decade (Table 1).

Data analysis

Our data analysis focused on two objectives: 1) evaluate the effectiveness of each method to provide useful, accurate data, and 2) use all the data collected to develop the best characterization of the inorganic layers in terms of their spatial and temporal distribution.

Comparison of analytical techniques

Visual stratigraphy, loss on ignition (LOI), total organic carbon (TOC), magnetic susceptibility, and gray-scale density were used to identify the location and type of sediments within the cores. Although the data sets are similar, each method measures a different physical or biochemical property of the sediment with varying resolution and sensitivity, resulting in slightly different records of inorganic layer location and thickness within the gyttja (Figure 5). LOI values (a proxy for % organic matter) have a strong positive correlation ($R^2 = 0.92$), with TOC values (% organic carbon; Figure 6). Comparison between quantitative data sets show that changes in organic matter content, as identified by LOI and TOC, are generally accompanied by changes in magnetic susceptibility and gray-scale density (Figure 5). We consider records of organic carbon content (LOI and TOC) as the most representative quantitative dataset for determining inorganic layer location and thickness, and use the litho-stratigraphic logs and X-radiographs to increase the resolution of the LOI and TOC records to include millimeter-scale laminations.

Core correlation

Correlation of the four cores from Ritterbush Pond permits determination of the lateral extent and lithologic variability of the inorganic sediments (Figure 7). The inorganic layers are less frequent in the upper and middle portions of the cores, and appear to cluster within particular intervals of each core. Three clusters of inorganic layers can be identified in each of the cores. Although the number and distribution of the layers vary within each cluster, it is possible to correlate the thickest graded beds among cores. Using the graphic logs and 5-point running average LOI records, we made a stratigraphic correlation between core C2 and the three other cores. The inorganic layers (low LOI values, or troughs) identified in C2 account for all significant troughs in the other cores, although one large trough in C2 may be represented as two closely spaced, smaller troughs in another core. Thick graded beds are present in all four cores and show thickness variations of up to 4 cm for correlative layers between cores.

We subdivided core C2 into six intervals, each noted by a Roman numeral based on the location and clustering of the inorganic layers (Figure 5,7). These intervals are common to all cores and the depth of the intervals is determined for cores C3, C4, and RT-2 by stratigraphic correlation. Even-numbered intervals (II, IV, VI) contain the lowest LOI values and the thickest inorganic layers, whereas odd-numbered intervals (I, III, V) have higher average LOI values with fewer and thinner inorganic layers.

Fourteen radiocarbon ages from four stratigraphic horizons confirm that the litho-stratigraphic correlation proposed above is also a time-stratigraphic correlation (Table 2). These four horizons were chosen for dating because of the presence of a thick graded bed at the base of each trough and the coincidence of the trough with an interval boundary. The best estimates of the trough ages are averages of values from the base or within the lowest layer contained in the trough. The standard deviation of the best estimate (average age) is consistent with the statistical variability (1 sigma) associated with the individual radiocarbon ages.

Age modeling

Using the six intervals identified in all cores, and the best estimates of the bracketing ages for those intervals, we used the stratigraphy from core C2 to develop a model to estimate the age of each inorganic layer. In order to portray accurately changes in gyttja and inorganic layer accumulation, the age model is

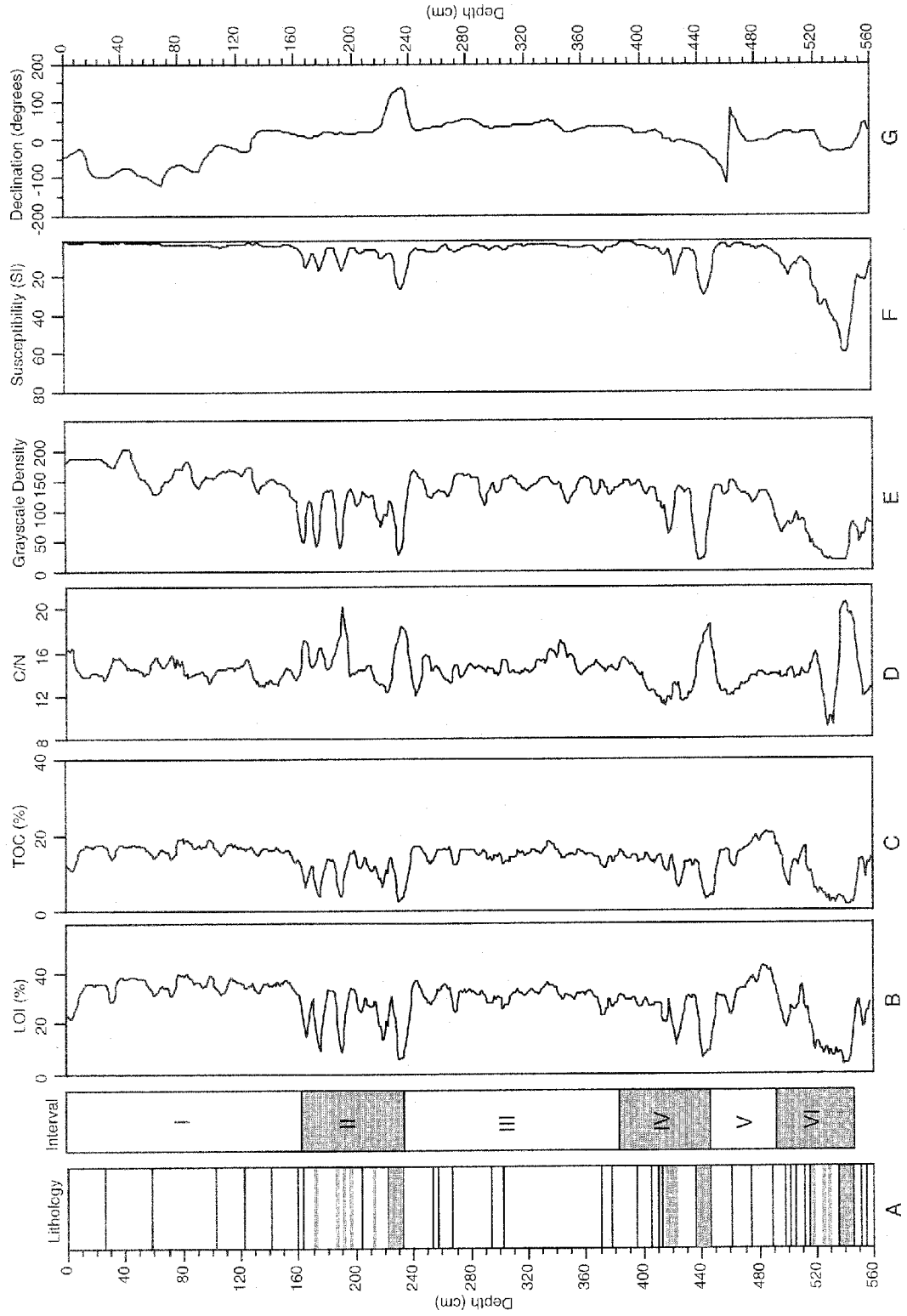

Figure 5. Comparison of high-resolution (centimeter by centimeter), whole core data sets on Ritterbush Pond core C-2 indicates location of inorganic layers (black in A). A: Lithology. White indicates predominantly gyttja and black indicates inorganic layers. B: Loss on ignition (LOI). C: Total organic carbon (TOC). D: Carbon:nitrogen ratio (C/N). E: X-radiograph gray-scale density. F: Magnetic susceptibility G. Paleomagnetic declination.

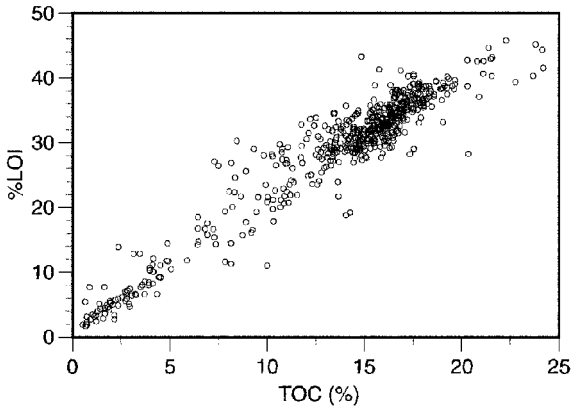

Figure 6. Comparison of LOI and TOC demonstrates a linear relationship ($R^2 = 0.92$) between datasets. TOC values are approximately 53% of LOI values for core C2.

based on the background accumulation of gyttja alone. We systematically removed the inorganic layers from the stratigraphy (Figure 8) according to distinct changes in lithology as identified by TOC data at 1-cm intervals. The model is insensitive to layers <5 mm, although the ages of the thin layers were calculated after age model construction. The virtual removal of the inorganic layers shortens the resulting apparent core length by 67 cm. Depth for each centimeter of the core length is recalculated as model depth to denote the removal of the inorganic layers (Table 3).

We use calibrated radiocarbon ages at the top and bottom of each interval to calculate an age for each centimeter of gyttja within that interval (Figure 9). Gyttja accumulation is modeled as linear between the upper and lower control points for each interval. Each inorganic layer, represented by an unconformity within the gyttja model, was assigned the age of the centimeter below the unconformity, a maximum age for the depositional event. Millimeter-scale laminations identified by lithostratigraphic logs and X-radiographs, but too thin to be removed from the stratigraphy during age modeling, are included in the event chronology and given the age of the centimeter of surrounding gyttja.

Radiocarbon-dated samples from the middle of intervals I, III and IV were used to check agreement

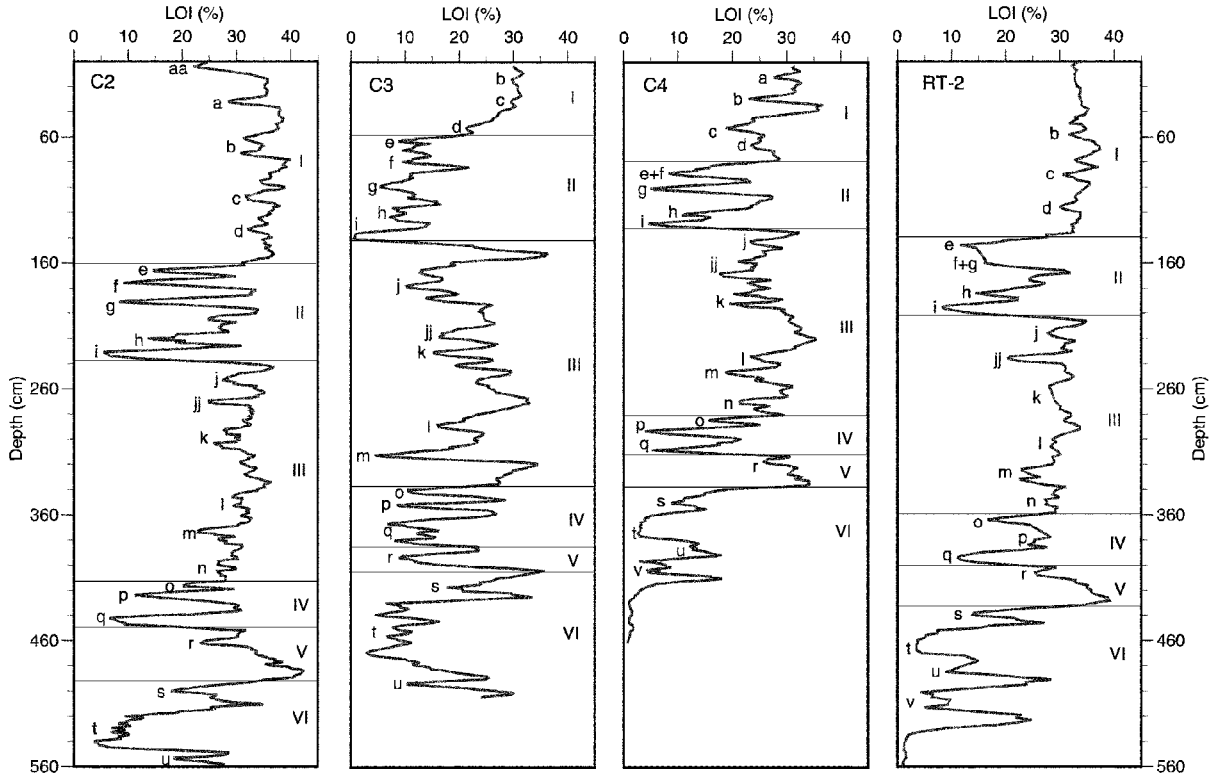

Figure 7. Correlation of Ritterbush Pond cores using smoothed (5-point running averages) LOI data. Lettered troughs indicate stratigraphic correlation between cores. Roman numerals indicate the division of each core into six intervals. Cores RT-1 and RT-2 LOI data from Bierman et al. (1997).

Table 2. Calibrated radiocarbon ages for Ritterbush core correlation.

Trough	CAMS #	Core	Depth	Sample	Position in trough	Calibrated age (yr BP)	Age in relation to base of trough	Best estimate of trough age ($\pm 1\sigma$)
e	33132	RT-2	96	gyttja	above first 2 layers	2090	younger	2020 ± 60
	44693	C3	63.5	wood	above second of 3 layers	1990	younger	
	44694	C4	81	leaves	above the only layer	1980	younger	
i	33352	RT-2	154	gyttja	base	2610	same	2620 ± 10
	44695	C3	154	wood	base (in layer)	2610	same	
	44696	C4	132	leaves	base (in layer)	2630	same	
q	20194	RT-2	348	gyttja	base	6820	same	6840 ± 30
	40775	C2	440	twig	in the only layer	6870	same	
	44697	C3	375	wood	base of second 4 layers	6630	younger (minimum)	
	44698	C4	311	gyttja	base	6820	same	
t	32854	RT-2	426	gyttja	base	9440	same	9440
	40776	C2	548	gyttja	1 cm below base	9510	older (maximum)	
	44699	C3	444	bark	top of the third of 8 layers	8580	younger (minimum)	
	44700	C4	380	wood	base	9440	same	

with the modeled age. In interval III, the age offset for the 275 cm model depth (C2 300 cm depth) is 80 years. A sample from interval IV at the 395 cm model depth (C2 424 cm depth) is also offset 80 years, which is within the analytic uncertainty for the radiocarbon ages. The offset was greater (200 years) in the unconsolidated top of the core (interval I).

Discussion

We investigated the mode of layer emplacement for the 52 inorganic layers identified in the Ritterbush Pond cores based on the physical, lithological, and isotopic data gathered on individual layers within the sediment cores. The inorganic layer (layer i) denoting the base of interval II (228–238 cm depth) in core C2 was chosen as representative of the thicker graded beds in all of the cores and was investigated using all available analytical techniques (Figure 10). These data are used to constrain the interpretation of possible emplacement mechanisms for layer i and other inorganic layers.

Physical characteristics

Layer i, measured visually, extends from 228 to 238 cm depth, with distinct upper and lower boundaries and internal grading. LOI, TOC, and grayscale density values confirm a 2-cm transition from gyttja to silt at the base of the layer, a well-mixed middle part, and an abrupt change from silt back to gyttja at the top (Figure 10). These data suggest that deposition of the inorganic layers involves intial mixing of gyttja and silt followed by deposition of relatively organic-free homogenous sand and silt, and then a return to gyttja deposition with little or no mixing at the layer top.

Grain size in layer i generally increases with depth, confirming the visual identification of the layer as a graded bed of coarse to fine silt. The upward decrease in grain size is interrupted at 234 cm depth by 3 cm of coarser sediment. The grading continues at 231 cm depth with significantly finer material in the top 1 cm. Graded beds are deposited by the suspension settling of particles, the grain size of which is determined by the available sediment and the energy of the moving water. For this same event, grain size in Core 3, taken close to the lake margin, is significantly coarser than in cores 2 and 4, located closer to the lake center. This decrease in grain size with distance from shore suggests deposition by a decelerating current carrying sediment toward the center of the lake.

Source of organic matter

Stable carbon isotope ($\delta^{13}C$) values become less negative with the transition from gyttja to silt, indicating a change in organic material from aquatic to terrestrial origin (Figure 10). This observation is supported by the visual identification of leaves, wood, and other terrestrial macrofossils within the inorganic layers. The upper transition from silt back to gyttja is sharper than the lower transition, supporting the hypothesis that the deposition of the inorganic layers involves mixing with gyttja at the base, but not at the top. The $\delta^{13}C$ values that fall in the range between

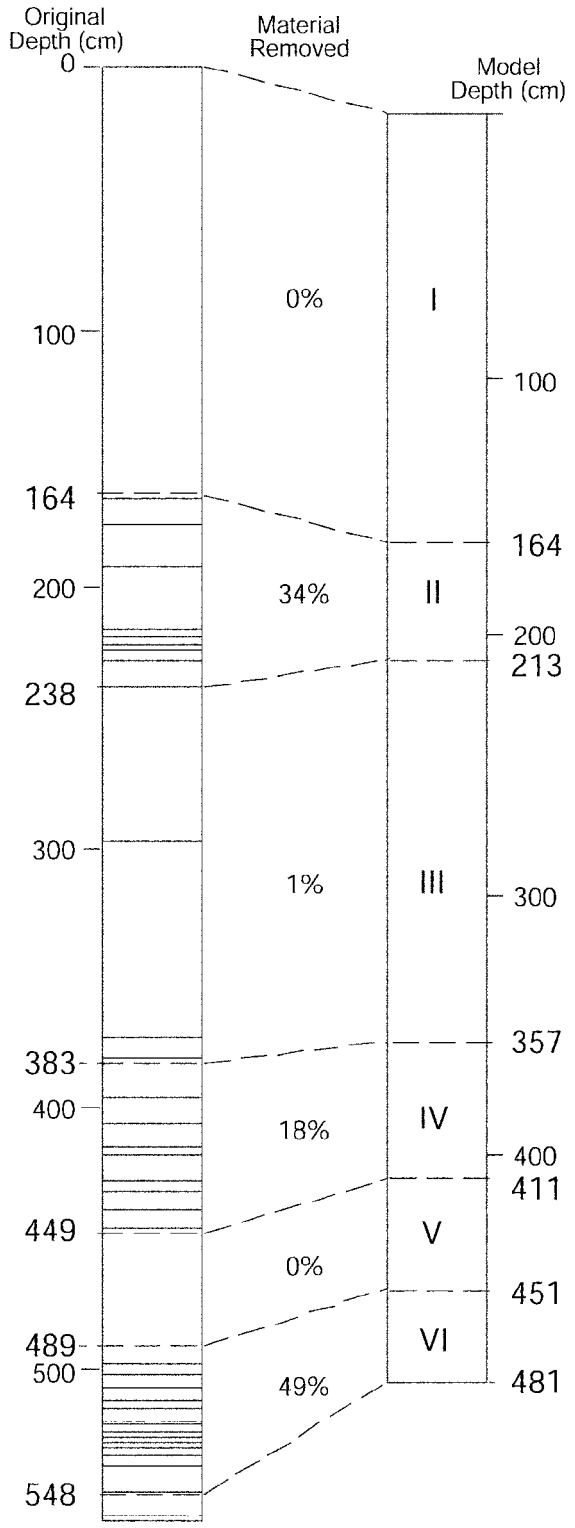

Figure 8. Compression of core C2 for age modeling. Layers representing rapid deposition are removed (12% decrease in total length) from the stratigraphy based on identification by graphic logs, pictures, TOC, and X-radiographic data.

gyttja values (−31‰) and the terrestrial (macrofossil) values (−28‰) for Ritterbush Pond (Bierman et al. 1997) could also result from a third source of organic material, such as macrophytes, or previously mixed terrestrial and aquatic material that is incorporated into the base of the layer.

C/N ratios support a terrestrial origin for the organic material in the inorganic layers, with C/N increasing from 15 to 20 toward 234 cm depth, 1 cm below the center of the layer. The C/N values show a 2-cm transition to higher (terrestrial) values at the base, and a jump to lower (aquatic) values 1 cm below the visually identified top of the layer. The change in organic matter source from aquatic to terrestrial in this layer suggests that material was delivered to the lake from the surrounding hillslopes or lake margins. The data available do not allow us to distinguish between terrestrial and lake marginal (emergent macrophytes) as sources of organic material with high C/N and depleted ^{13}C.

Charcoal data

The susceptibility of the hillslopes to erosion is increased by forest fires that strip protective and stabilizing vegetation (Clark (1988); Meyers et al. 1995). In Rittersbush Pond sediments, there is a decrease in charcoal abundance within the inorganic layers compared to the surrounding gyttja (Figure 10). Although this observation does not exclude the possibility that fires occurred in the surrounding watershed and contributed sediment to the pond, charcoal data do not support widespread, hillslope-clearing fires as a trigger for inorganic layer deposition.

Timing of layer deposition

Samples previously analyzed (Bierman et al. 1997) in core RT-2 for radiocarbon include gyttja samples above and below three inorganic layers (i, q, and t) that have been correlated to core C2. Each of the three pairs exhibits an inversion in age; the radiocarbon age above the layer is slightly but consistently older than the age below the layer. For layer i the offset is 180 cal. yr, for layer q 100 cal. yr, and for layer t the offset is 200 cal. yr. As the offset is not within the analytic uncertainty of the radiocarbon ages (1 sigma), and is systematic for each of the thickest, graded inorganic layers in the core, the offset is probably a characteristic of the mechanism that deposited the inorganic layers.

Table 3. Modeled Layer Age in Radiocarbon and Calendar Years for Core, C2

Interval	Trough[1]	Layer[2]	Core depth (cm)	Thickness[3] (cm)	Model depth	Model age (^{14}C yr BP)	Model age (cal yr BP)	Time since last event (cal yr)
I	aa	1	4–5	1	5	63	62	319
	a	2	30.8–31.0	0.2	31	391	381	382
		3	61.0–61.2	0.2	62	781	763	160
	b	4	74.6–74.8	0.2	75	945	923	356
	c	5	103.8–104.0	0.2	104	1310	1279	259
		6	124.7–124.9	0.2	125	1575	1538	221
	d	7	142–143	1	143	1802	1759	209
II	e	8	159.0–159.2	0.2	160	2016	1968	57
		9	164–167	3	165	2081	2025	73
	f	10	173–177	4	171	2139	2098	134
	g	11	188–193	5	182	2244	2232	122
	h	12	203–204	c (0.2)	192	2340	2354	159
		13	217–219	2	205	2465	2513	24
		14	221–222	1	207	2484	2537	25
		15	224.0–224.2	0.2	209	2503	2562	58
	i	16	228–237	9	213	2540	2620	333
III	j	17	254.5–254.7	0.2	230	2800	2953	81
		18	258.5–258.7	0.2	234	2862	3034	241
	jj	19	270.5–271.0	0.5	246	3050	3275	523
	k	20	296.0–296.3	0.3	272	3455	3798	60
		21	305.0–305.5	0.5	280	3502	3858	181
		22	309.4–309.5	0.1	284	3642	4039	201
		23	319.0–319.1	0.1	294	3798	4240	723
	l	24	355.0–355.1	0.1	330	4360	4963	61
		25	358.0–358.1	0.1	333	4407	5024	261
	m	26	371.8–372.0	0.2	346	4610	5285	40
		27	373.0–373.2	0.2	348	4641	5325	141
		28	380.0–380.3	0.3	355	4750	5466	404
IV		29	397.8–397.9	0.1	372	5107	5870	220
	n	30	406.2–406.7	c (0.1)	381	5305	6090	97
		31	411.3–411.4	0.1	385	5393	6187	147
	o	32	415.2–416.0	0.8	391	5525	6334	97
	p	33	420–423	3	395	5613	6431	74
		34	426.5–426.6	0.1	398	5679	6505	122
		35	431.8–431.9	0.1	403	5789	6627	213
	q	36	439.5–449.0	9.5	411	5980	6840	441
V	r	37	461.1–461.8	c (0.2)	423	6388	7281	414
		38	477.5–477.7	0.2	439	6905	7695	476
VI	s	39	492–493	c (0.3)	454	7373	8171	282
		40	497.4–497.6	0.2	460	7609	8453	141
		41	501–502	1	463	7727	8594	188
		42	506–508	2	467	7884	8782	141
		43	511.5–511.6	0.1	468	8002	8923	47
		44	512.6–512.7	0.1	471	8041	8970	47
	t	45	513–514	1	472	8080	9017	94
		46	516.0–516.1	0.1	473	8159	9111	47
		47	517.5–520.0	2.5	475	8198	9158	47
		48	521–522	1	476	8238	9205	47
		49	523–525	2	477	8277	9252	47
		50	526–532	c (1.5)	478	8316	9299	94
		51	533–535	2	479	8395	9393	47
		52	537–547	10	481	8434	9440	235[4]

[1]as identified in Core, C2

[2]layers identified by litho-stratigraphic logs, X-radiographs, and TOC

[3] c = couplet, layer thickness in ()

[4]estimated from lithostratigraphic logs and accumulation rate of interval VI

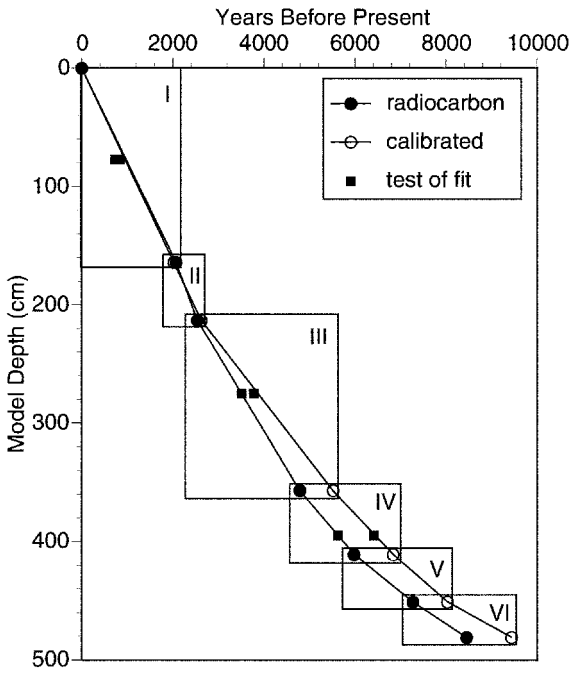

Figure 9. Age model for Ritterbush Pond Core 2. Accumulation rate is modeled as linear between age control points (circles). Linear modeling was tested by independently radiocarbon dating samples from intervals I, III, and IV (squares).

The inversion of the ages suggests that there is both erosion and deposition associated with the mechanism emplacing the inorganic layers. Bierman et al. (1997) propose initial scouring of lake sediments by turbidity currents at the lake margins, followed by deposition of the graded bed, and then redeposition of the disturbed lake sediment on top of the inorganic layer. At the lake center, where the inversion is observed, the scouring would erode less sediment than at the lake margins; the net movement of the disturbed sediments toward the center of the lake creates the measured offset in age. The resuspension and redeposition of sediment within a lake basin, termed sediment focusing, may result in higher net rates of gyttja accumulation in the lake center than at the lake margins (Davis et al. 1984; Hilton 1985; Lehman 1975). The minor age inversion surrounding the inorganic layers in Ritterbush Pond is probably due to discreet, episodic, sediment focusing events that rework older, lake marginal material and create a measurable disturbance in the temporal sequence. A similar age inversion was observed in the gyttja above tsunami deposits (Bondevik et al. 1997); the gyttja was 300–500 ^{14}C yr older than the material below and within the tsunami deposit. The offset was interpreted to be the post-tsunami reworking of older material exposed by tsunami scouring at the edges of the coastal lake basin.

Layer emplacement mechanisms

Together, the lithologic, isotopic, radiocarbon, and grain size data suggest that the following criteria must be met by inorganic layer emplacement mechanism(s): 1) rapid deposition of terrestrial material from suspension (grain size data), 2) possible gyttja scouring and mixing with inorganic material at the base of the deposit (LOI, C/N, δ^{13}C data), 3) fining of the deposit toward the center of the lake (grain size data), 4) deposition of both fine laminations and thick ($>$1 cm) layers (stratigraphy), and 5) age inversion (^{14}C data). Mechanisms associated with event sedimentation in lakes include, but are not limited to: turbidity currents (density currents with a high concentration of dispersed sediment), plumes of sediment that undergo suspension setting or evolve into density-driven bottom currents, the reworking of lake marginal sediment by storm-(wind or wave) generated bottom currents, and slumping of lake marginal or hillslope sediments (Gorsline 1984). Density-driven bottom currents and high-concentration turbidity currents are most likely to result in the set of characteristics observed in the thickest inorganic layers. There is not sufficient evidence to determine if a single type of current (or more than one) is responsible for deposition of layers in Ritterbush Pond.

Spatial distribution of inorganic layers

The variation in thickness and grain size of the inorganic layers within each core is probably due to changes in sediment source location, sediment availability, and the velocity of sub-aqueous currents transporting sediment. The distance of the core location from the sediment source (e.g., stream or lake marginal slump) for each individual layer will influence layer thickness and mean grain size; the closer and more active the sediment source, the coarser and thicker the deposit. In core C2, inorganic layers composed of similar grain sizes range from 1 to 10 cm thick. The thicker layers may result from a larger amount of sediment available for transport or a greater magnitude (duration and intensity) hydrologic event. Inorganic laminations ($<$5 mm thick) tend to be finer grained than thicker layers, suggesting lower transport

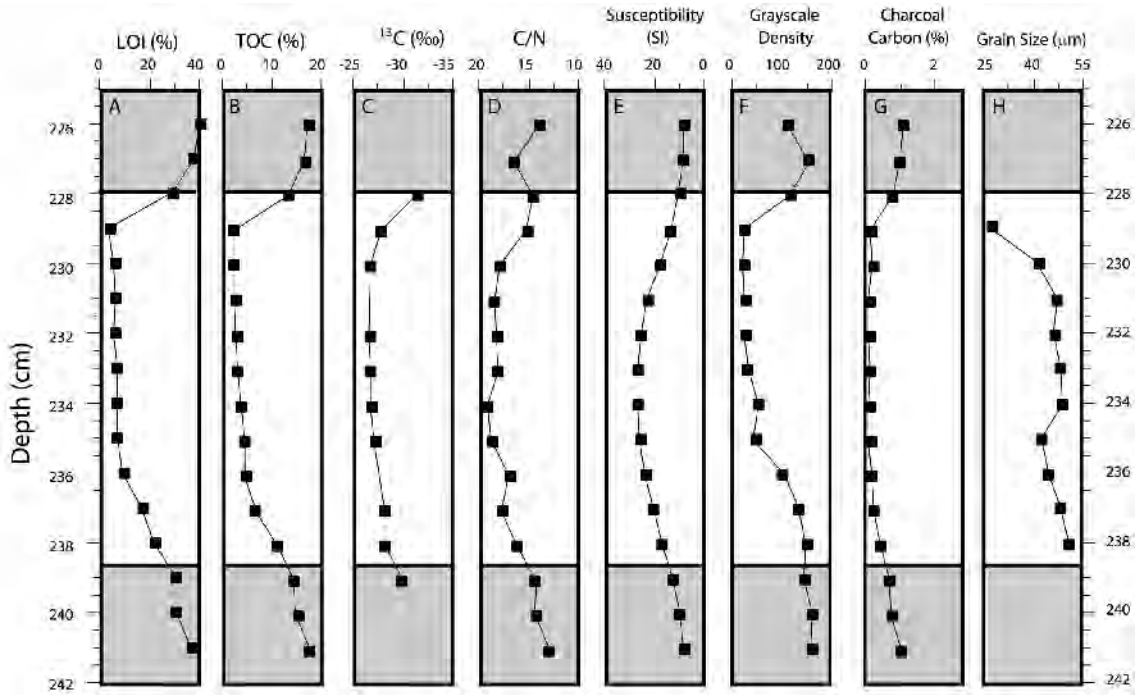

Figure 10. Summary data for layer deposition using Core 2, layer i. Shifts to terrestrial material are to the left (white background); shifts to the right indicate aquatic material (shaded background). Radiocarbon dated gyttja above (2720 ^{14}C ybp) and below (2490 ^{14}C ybp) the inorganic layer exhibit age inversion. A. Loss on ignition (LOI) B. Total organic carbon (TOC) C. Stable carbon isotope (δ^{13}C) D. Carbon:nitrogen (C/N) E. Magnetic susceptibility F. Grayscale density G. Charcoal carbon H. Grain size.

velocity and a smaller magnitude sediment transport event.

Temporal distribution of inorganic layers

The Ritterbush event chronology shows non-random fluctuation in layer thickness and distribution over time (Table 3, Figure 11). The layers (>5 mm) are present in three distinct clusters; the laminations (<5 mm) are more evenly distributed. In the intervals where the inorganic layers cluster, the thickest layer is consistently at the base of the interval. Subsequent layers decrease in relative thickness in each of the intervals. Although event data are unavailable previous to 9500 cal years BP, LOI records for cores RT-2 and C-4 suggest at least one additional event above the till and outwash associated with deglaciation of the basin (>12,900 cal yr BP). Therefore, the lowest layer in the event chronology may not be the base of interval VI.

From 9500 to 8500 cal yr BP, there are eight inorganic layers and four laminations, deposited every 50 to 190 years, the highest concentration of layers in the record. There are only two single laminations, and two fine couplets, spaced 210 to 480 years apart, prior to the next cluster of layers beginning at 6750 cal yr BP (interval IV). This cluster consists of three layers and two laminations deposited 70 to 150 years apart. From 6250 to 2750 cal yr BP (interval III), 14 laminations and one couplet occur 40 to 720 years apart. The next cluster of layers, from 2750 to 2000 cal yr BP (interval II), contains six layers, two laminations and two couplets that were deposited 20 to 160 years apart. The frequency of deposition decreases again in interval I, where only one layer and six laminations were identified, ranging 160 to 380 cal yr apart. The youngest inorganic layer identified, estimated at 62 cal yr BP, is a diffuse centimeter of macrofossil-rich sand, and is the only evidence of event deposition in the last 300 years. This event is consistent with the 1927 flood of record (Brown et al. 2000).

Implications of findings

The Ritterbush Pond cores provide a detailed record of discrete sedimentation events. The sand and silt

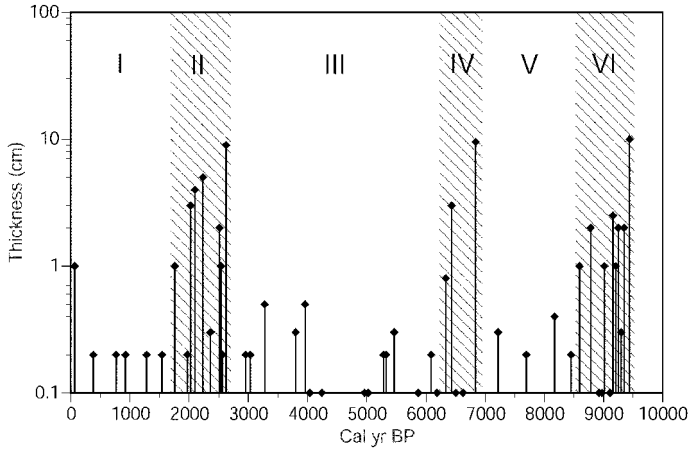

Figure 11. Event chronology based on calibrated ^{14}C ages for organic material from Ritterbush Pond. Thickest and most frequent layer deposition is clustered in three shaded intervals (II, IV, VI) during the late, middle, and early Holocene.

layers are terrestrially-derived and transported from the lake margins toward the lake center, probably by density currents. As charcoal data do not support hillslope-clearing fires as a triggering mechanism, and because the Ritterbush watershed is not located in an active seismic zone, the transport of sediment to the lake is most likely caused by episodic increases in stream flow, which erode stream channels, stream banks, and lake margins (Brown et al. 2000).

Patterns in temporal distribution of inorganic layers

The temporal distribution of the inorganic layers suggests changing basin-wide sedimentation dynamics since deglaciation over 12,000 years ago; specifically, there were three 400- to 1000-year long periods where the frequency and thickness of the layers increased. The average recurrence interval for sedimentation events in odd intervals (low-magnitude and frequency events) is 270 $\pm$ 170 cal yr BP, and the average event recurrence for even intervals (high magnitude and frequency events) is 130 $\pm$ 100 cal yr BP. The more frequent event recurrence during the even-numbered intervals suggests periodic changes in the frequency of terrestrial sediment delivery to the lake during the Holocene. The paucity of large depositional events during the thousands of years separating these three active intervals suggests that the frequency of layer deposition may be influenced by fluctuations in regional climate and hydrology.

In the northeastern United States, general trends in average precipitation, temperature, and vegetation since deglaciation have been reconstructed using specific pollen abundance as a climate proxy record (Jackson and Whitehead 1991; Spear et al. 1994). Although the exact timing varies, all proxy records suggest a gradual rise in temperature following deglaciation, maximum warmth in the mid-Holocene (the Hypsithermal), and cooling toward present climate conditions (Davis 1969). The wettest period of the Holocene, as interpreted from lake-level curves (Webb et al. 1993), occurred from 8000 to 6000 ^{14}C yr BP. The pollen chronology for Ritterbush Pond (Lin 1996) suggests warm, moist conditions from 9000 to 1600 ^{14}C yr BP, spanning all three intervals of increased deposition of inorganic layers.

The lack of correspondence between intervals of increased layer deposition with any particular climate regime suggests that the increase in terrestrial sediment delivery to the lake is not necessarily caused, or accompanied, by changes in average climate conditions, primarily mean annual precipitation and temperature, which control watershed vegetation assemblages. If the increased frequency of layer deposition indicates a prolonged period (up to 1000 years) of increased precipitation, the change should be reflected by a shift in vegetation; such a change is not seen in the pollen record. However, a series of high-magnitude storm events would increase the frequency of saturated overland flow, stream channel erosion, and terrestrial sediment delivery to the lake, without impacting the watershed sufficiently to cause vegetation changes detectable by pollen analysis.

Ritterbush Pond morphology

The physical characteristics of Ritterbush Pond strongly influence the sensitivity of the hillslopes and stream channels to erosion. Similar to other Vermont lakes, the watershed is forested, relatively small, and has significant bedrock outcrops. In contrast to many other ponds, Ritterbush Pond has steep hillslopes with average gradients of 20% to 60%, on all sides. Although the vegetation in the watershed limits hillslope erosion and mass movement during moderate hydrologic events, the steep slopes increase the velocity of runoff once the ground is saturated, maximizing the potential for channel scouring and bank erosion. The gravel deposits near Big Muddy Pond may be a significant source of easily scoured sediment, transported to Ritterbush Pond during high-magnitude runoff events.

Once sediment reaches Ritterbush Pond, potential for preservation is enhanced by lake bathymetry. Unlike the gentle, shallow bathymetry of some ponds in Vermont that show few or no distinct layers (Gran et al. 1999; Lin 1996), Ritterbush Pond has a deeper bowl-shaped basin. The movement of sediment stored at the shallow margins, where streams lose competence and build deltas, toward the deep flat center of the lake is facilitated by steep inner-lake slopes conducive to sediment resuspension and density-current transport. Additionally, the steep inner slopes of the lake minimize the removal of material from the lake center once it has been deposited. Shallower basins with lower outlets could experience resuspension and transport of fine-grained sediment from the lake during periods of high discharge.

Development of additional records

In other areas of the world, episodic inorganic sediment deposition has recently received increased attention as a climate proxy. Changes in the frequency, grain size, and thickness of inorganic deposits in lake sediments have been used to interpret changes in local sedimentation dynamics and compared with global climate records (Lamy et al. 1998; Rodbell et al. 2000; Moscaiello et al. 1998; Cooper and O'Sullivan 1998). Layers of inorganic sediment have been used to determine the frequency of monsoons in the South China Sea (Huang et al. 1997) and storms in Canada (Campbell 1998) and New Zealand (Eden and Page 1998). Many of these records have been explained by regional and global climate patterns, such as ENSO events, and changes in atmospheric and oceanic circulation. This paper demonstrates that in New England lacustrine sediment records allow for the detection of short term climate changes not preserved in other proxy records such as pollen. In particular, our analysis of sediment cores allows reliable detection of stormy intervals in the Holocene (Brown et al. 2000).

Acknowledgements

Supported by grants to Brown from the University of Vermont Graduate College, Vermont Geological Society, Sigma Xi, a Geological Society of America Research Grant and Howard Award. Supported by National Science Foundation Career grant EAR-9702643 (Bierman) and instrumentation grant EAR-9724190 (Bierman and Lini). Radiocarbon measurements supported in part by U.S Department of Energy contract W-7405-ENG-48. We thank faculty and students at the University of Vermont for field assistance, Killian for LOI measurements (RT-1 and RT-2), Rodbell for grain size analysis, and King and Peck for paleomagnetics.

References

Babcock R.D. 1979. Soil Survey of Lamoille County, Vermont. USDA: 43 pp.

Bierman P., Lini A., Zehfuss P., Church A., Davis P.T. and Southon J. 1997. Postglacial ponds and alluvial fans: Recorders of Holocene landscape history. GSA Today 7: 1–8.

Bondevik S., Svendsen J.I., Johnse G., Mangerud J. and Kaland P.E. 1997. The Storegga tsunami along the Norwegian coast, its age and runup. Boreas 26: 29–53.

Brown S.L., Bierman P.R., Lini A., Davis P.T. and Southon J. 2000. 10 000 yr record of extreme hydrologic events. Geology 28: 335–338.

Campbell C. 1998. Late Holocene lake sedimentology and climate change in Southern Alberta, Canada. Quat. Res. 49: 96–101.

Clark J.S. 1988. Stratigraphic analysis on petrographic thin sections: Application to fire history in northwest Minnesota. Quat. Res. 30: 81–91.

Cooper M.C. and O'Sullivan P.E. 1998. The laminated sediments of Loch Ness, Scotland: Preliminary report on the construction of a chronology of sedimentation and its potential use in assessing Holocene climatic variability. Palaeogeogr. Palaeoclim. Palaeoecol. 140: 23–31.

Davis M.B. 1969. Climatic changes in southern Connecticut recorded by pollen deposition at Rogers Lake. Ecology 50: 409–422.

Davis M.B., Moeller R.E. and Ford J. 1984. Sediment focusing and pollen influx. In: Hayworth E.Y. and Lund J.W.G. (eds), Lake

Sediments and Environmental History. University of Minnesota Press, Minneapolis, pp. 261–294.

Davis P.T. 1999. Cirques of the Presidential Range, New Hampshire, and surrounding alpine areas in northeastern United States. Geographie Phys. Quat. 53: 24–45.

Davis R.B. and Jacobson G.L. Jr. 1985. Late glacial and early Holocene landscapes in northern New England and adjacent areas of Canada. Quat. Res. 23: 341–368.

Donahue D.J., Linick D.W. and Jull A.J.T. 1990. Isotope ratio and background corrections for accelerator mass spectrometry radiocarbon measurements. Radiocarbon 32: 135–142.

Eden D.N. and Page M.J. 1998. Paleoclimatic implications of a storm erosion record from late Holocene lake sediments, North Island, New Zealand. Palaeogeogr. Palaeoclim. Palaeoecol. 139: 37–58.

Gorsline D.S. 1984. A review of fine-grained sediment origins, characteristics, transport and deposition. In: Stow D.A.V. and Piper D.J.W. (eds), Fine-grained Sediments: Deep-water Processes and Facies. Blackwell Scientific Publications, Oxford Geological Society Special Publication No. 15., pp. 17–34.

Gran S., Nichols K. and Bierman P.R. 1999. Teaching winter geohydrology using frozen lakes and snowy mountains. J. Geosci. Ed. 47: 420–427.

Hilton J. 1985. A conceptual framework for predicting the occurrence of sediment focusing and sediment redistribution in small lakes. Limnol. Oceanogr. 30: 1131–1143.

Huang C.Y., Liew P.M., Zhao M., Chang T.C., Kuo C.M. and Chen M.T. 1997. Deep sea and lake records of the Southeast Asian paleomonsoons for the last 25 thousand years. Earth Planet. Sci. Lett. 146: 59–72.

Jackson S.T. and Whitehead D.R. 1991. Holocene vegetation patterns in the Adirondack Mountains. Ecology 72: 641–653.

Lamy F., Hebbeln D. and Wefer G. 1998. Late Quaternary precessional cycles of terrigenous sediment input off the Norte Chico, Chile, and palaeoclimatic implications. Palaeogeogr. Palaeoclim. Palaeoecol. 141: 233–251.

Lehman J.T. 1975. Reconstructing the rate of accumulation of lake sediment: The effect of sediment focusing. Quat. Res. 5: 541–550.

Lin L. 1996. Environmental changes inferred from pollen analysis and ^{14}C ages of pond sediments, Green Mountains, Vermont. University of Vermont, Burlington, 125 pp.

Lini A., Bierman P.R., Lin L. and Davis P.T. 1995. Stable carbon isotopes in post-glacial lake sediments: A technique for timing the onset of primary productivity and verifying AMS ^{14}C dates. GSA Abstracts with Programs: A-58.

Lund S.P. 1996. A comparison of Holocene paleomagnetic secular variation records from North America. J. Geophys. Res. 101: 8007–8024.

Moscaiello S., Schneider A.M. and Filippi M.L. 1998. Late glacial and early Holocene palaeoenvironmental changes in Geneva Bay. Palaeogeogr. Palaeoclim. Palaeoecol. 140: 51–73.

Meyers G.A. and Wells S.G. 1997. Fire-related sedimentation events on alluvial fans, Yellowstone National Park, USA. J. Sed. Res. 67: 776–791.

Olsson I.U. 1986. Radiometric dating. In: Stow D.A.V. and Piper D.J.W. (eds), Fine-grained Sediments: Deep-water Processes and Facies. Blackwell Scientific Publications, Oxford Geological Society Special Publication No. 15., pp. 273–297.

Peck J.A., King J.W., Colman S.M. and Kravchinsky V.A. 1996. An 84-kyr paleomagnetic record from the sediments of Lake Baikal, Siberia. J. Geophys. Res. 101: 11365–11385.

Reasoner M.A. 1993. Equipment and procedure improvements for a lightweight, inexpensive, percussion core sampling system. J. Paleolim. 8: 273–281.

Ridge J.C., Besonen M.R., Brochu M., Brown S., Callahan J.W., Cook G.J. et al. 1999. Varve, paleomagnetic, and 14C chronologies for late Pleistocene events in New Hampshire and Vermont. Geographie Phys. Quat. 53: 79–106.

Rodbell D.T., Seltzer G.O., Anderson D.M., Abbott M.B., Enfield D.B. and Newman J.H. 2000. An ~15,000-year record of El-Nino driven alluviation in southwestern Ecuador. Science 283: 516–520.

Spear R.W. 1989. Late Quaternary history of high-elevation vegetation in the White Mountains of New Hampshire. Ecol. Mon. 59: 125–151.

Spear R., Davis M.B. and Shane L.C. 1994. Late Quaternary history of low- and mid-elevation vegetation in the White Mountains of New Hampshire. Ecol. Mon. 64: 85–109.

Sperling J.A., Wehrle M.E. and Newman W.S. 1989. Mountain glaciation at Ritterbush Pond and Miller Brook, northern Vermont, reexamined. Northeastern Geology 11: 106–111.

Stuiver M. and Polach H.A. 1977. The reporting of ^{14}C data. Radiocarbon 19: 355–363.

Stuiver M. and Reimer P. 1993. Extended ^{14}C database and revised CALIB 3.0 ^{14}C age calibration program. Radiocarbon 35: 215–230.

Thompson W.B, Fowler B.K., Flanagan S.M. and Dorian C.C. 1996. Recession of the late Wisconsinan ice sheet from the northwestern White Mountains, New Hampshire. In: Van Baalen M.R. (ed.), Guidebook to Field Trips in Northern New Hampshire and Adjacent Regions of Maine and Vermont. Harvard Printing and Publications, Cambridge, pp. 203–234.

Webb T., Bartlein P.J., Harrison S.P. and Anderson K.J. 1993. Vegetation, lake-levels, and climate in eastern North America for the past 18000 years. In: Wright H.E. (ed.), Global Climates Since the Last Glacial Maximum. University of Minnesota Press, Minneapolis, pp. 415–467.

Winkler M.G. 1985. Charcoal analysis for paleoenvironmental interpretation: A chemical assay. Quat. Res. 23: 313–326.

Wohlfarth B., Bjorck S., Possnert G., Lemdahl G., Brunnberg L., Ising J. et al. 1993. AMS dating Swedish varved clays of the last glacial/interglacial transition and the potential difficulties of calibrating Late Weichselian 'absolute' chronologies. Boreas 22: 113–128.